Research Square

Preprints are preliminary reports that have not undergone peer review.
They should not be considered conclusive, used to inform clinical practice,
or referenced by the media as validated information.

# Value of Contrast-Enhanced Ultrasound Arrival-Time Parametric Imaging for Differentiating Hepatocellular Adenoma from Focal Nodular Hyperplasia

**Qingxin Li**
the First Hospital of Jilin University
**Xueyang Qin**
the First Hospital of Hebei Medical University
**Ying Sun**
the First Hospital of Jilin University
**Dongxuan Wang**
the First Hospital of Jilin University
**Mingwei Sui**
the First Hospital of Jilin University
**Yupeng Zhu**
the First Hospital of Jilin University
**Haibin He**
the First Hospital of Jilin University
**Qi Zheng**
the First Hospital of Jilin University
**Dezhi Zhang**
dezhi@jlu.edu.cn
the First Hospital of Jilin University

**Research Article**

**Keywords:** Contrast-Enhanced Ultrasound, Parametric Imaging, Focal Nodular Hyperplasia, Hepatocellular Adenoma, Differential Diagnosis

**Posted Date:** November 1st, 2026

**DOI:** https://doi.org/10.21203/rs.3.rs-11110387/v1

**License:** This work is licensed under a Creative Commons Attribution 4.0 International License.
Read Full License

**Additional Declarations:** No competing interests reported.

## Abstract

# Objective

Focal nodular hyperplasia (FNH) and hepatocellular adenoma (HCA) are benign hepatocellular lesions that may show overlapping imaging features but require different clinical management strategies. This study aimed to evaluate the value of arrival-time parametric imaging (ATPI) in differentiating HCA from FNH by characterizing lesion-specific early arterial enhancement patterns and vascular architecture.

# Materials and methods

In this retrospective study, 54 patients (36 FNH, 18 HCA) underwent CEUS between January 2020 and January 2024. Final diagnosis was based on histopathology or typical CT/MRI findings with ≥ 12 months follow-up. CEUS and ATPI features were analyzed, and diagnostic performance of CEUS alone versus CEUS combined with ATPI was compared. Interobserver agreement was assessed using Cohen's kappa.

# Results

FNH more frequently exhibited centrifugal enhancement, spoke-wheel arteries, and intralesional arterial branches, whereas HCA showed centripetal enhancement and prominent feeding arteries. Compared with CEUS alone, CEUS combined with ATPI improved sensitivity from 77.8% to 94.4%, specificity from 86.1% to 91.7%, accuracy from 83.3% to 92.6%, positive predictive value from 73.7% to 85%, and negative predictive value from 88.6% to 97.1%. Interobserver agreement increased from κ = 0.683 with CEUS alone to κ = 0.757 after ATPI was incorporated.

# Conclusion

ATPI may provide additional information on early arterial enhancement patterns and vascular architecture in FNH and HCA. Although CEUS combined with ATPI showed numerically higher diagnostic performance than CEUS alone, further studies with larger sample sizes are needed to confirm its incremental diagnostic value.

## Introduction

Focal nodular hyperplasia (FNH) is one of the most common benign solid liver lesions and occurs predominantly in young women[1]. It is generally considered not to be a true neoplasm, but rather a hyperplastic response of hepatic parenchyma to localized vascular abnormalities or altered hemodynamics. Histologically, classic FNH is characterized by a central stellate scar, radiating fibrous septa, and abnormal vascular structures[2]. Hepatocellular adenoma (HCA), in contrast, is a relatively

uncommon benign hepatocellular tumor that also occurs mainly in young to middle-aged women and is associated with risk factors such as oral contraceptive use, obesity, and metabolic dysfunction[3]. Although both FNH and HCA are benign focal liver lesions and may share overlapping epidemiological and imaging features, their clinical management differs substantially. FNH usually follows a stable clinical course and generally requires no specific treatment[4]. In contrast, HCA carries a potential risk of hemorrhage and malignant transformation, and some patients may require close surveillance, modification of hormonal or metabolic risk factors, interventional treatment, or surgical resection[5]. Therefore, accurate differentiation between FNH and HCA is essential for appropriate clinical decision-making.

Conventional ultrasound has limited value in distinguishing FNH from HCA because both lesions often show nonspecific sonographic features[6]. Contrast-enhanced ultrasound (CEUS) enables real-time assessment of lesion vascularity and perfusion dynamics; however, the enhancement patterns of FNH and HCA may overlap, particularly in atypical FNH without a clear spoke-wheel pattern or central scar and in hypervascular or heterogeneously enhancing HCA[7].

Arrival-time parametric imaging (ATPI) is derived from dynamic CEUS data and uses color coding to visualize differences in the arrival time of microbubble contrast agents within different regions of a lesion and the surrounding liver parenchyma[8]. This technique allows intuitive assessment of the temporal and spatial distribution of lesion perfusion[9]. By displaying the temporal and spatial distribution of perfusion, ATPI may reveal vascular characteristics that are not readily appreciated on conventional CEUS. Therefore, this study aimed to evaluate the role of ATPI in characterizing the microvascular perfusion patterns of FNH and HCA and to investigate its diagnostic value in differentiating these two lesions.

## Materials and Methods

# Participants

This retrospective study included patients who underwent liver CEUS at the First Hospital of Jilin University between January 2020 and January 2024 and were diagnosed with FNH or HCA. The final diagnosis was established either by histopathology or by typical findings on contrast-enhanced computed tomography (CECT) or gadoxetic acid-enhanced magnetic resonance imaging (EOB-MRI), with an imaging follow-up period of at least 12 months[10].

## Inclusion and Exclusion Criteria

The inclusion criteria were as follows: a final diagnosis of FNH or HCA confirmed by histopathology or established based on CECT or EOB-MRI findings with more than 12 months of imaging follow-up; no prior treatment before CEUS examination; and a lesion diameter between 1 and 5 cm that measured on

baseline ultrasound images. The exclusion criteria were as follows: lesions showing no enhancement throughout the CEUS examination; poor image quality caused by respiratory motion or other motion artifacts, which precluded ATPI analysis; target lesions that could not be clearly identified or reliably evaluated on CEUS images; and age younger than 18 years.

## CEUS

All ultrasound examinations were performed using a LOGIQ Fortis ultrasound system (GE Healthcare) equipped with CEUS and ATPI post-processing software. A C1-6 convex transducer was used, with a frequency range of 3.5–5.0 MHz. During CEUS, the mechanical index was set between 0.06 and 0.15. SonoVue (Bracco, Milan, Italy) was used as the ultrasound contrast agent.

After conventional ultrasound examination, CEUS was performed for the target liver lesion. The entire CEUS process was recorded continuously for subsequent analysis. During image acquisition, the transducer was kept as stable as possible, and patients were instructed to cooperate with breath-holding or shallow breathing to minimize motion artifacts[11]. The CEUS examination was continuously observed for at least 3–5 min after contrast injection. All CEUS examinations were performed by an experienced ultrasound physician and specialized training in liver CEUS.

## ATPI

ATPI was performed using arterial-phase CEUS cine clips. For each lesion, a 5-s video clip was selected beginning at the time when the contrast agent first arrived within the lesion, which was defined as 0 s. The selected CEUS clip was then processed using the built-in parametric imaging software of the ultrasound system to generate color-coded arrival-time parametric images[8]. The arrival time of the contrast agent within the lesion was encoded using different colors according to the temporal sequence of microbubble arrival. Earlier enhancement was therefore displayed in warmer colors, whereas delayed enhancement was displayed in cooler colors (Fig. 1). The ATPI analysis was performed by two independent readers who were blinded to the final diagnosis.

## Evaluation of Sonographic Features

All CEUS cine loops were reviewed frame by frame. The following CEUS features were assessed: time of enhancement onset, enhancement degree compared with adjacent liver parenchyma, enhancement homogeneity, enhancement direction, presence or absence of washout, and degree of washout. The enhancement degree was classified as hyperenhancement, isoenhancement, hypoenhancement, or nonenhancement. Enhancement homogeneity was classified as homogeneous or heterogeneous. Enhancement direction was classified as centrifugal, centripetal, or diffuse enhancement when applicable (Fig. 2).

The vascular and structural features of the lesions were also recorded, including the presence of a feeding artery (Fig. 3A), intralesional arterial branch (Fig. 3B), spoke-wheel artery (Fig. 3C), and central scar (Fig. 3D). A spoke-wheel artery was defined as an intralesional arterial structure radiating from the center toward the periphery, resembling the spokes of a wheel[12]. A feeding artery was defined as a relatively large arterial vessel entering the lesion from the surrounding liver parenchyma. An intralesional arterial branch was defined as an arterial branch extending from the feeding artery within the lesion. A central scar was defined as an intralesional nonenhancing area[11].

After ATPI processing, the enhancement pattern of each lesion was evaluated on color-coded images and classified as homogeneous, centrifugal, or centripetal enhancement (Fig. 4). The presence of a feeding artery, intralesional arterial branch, spoke-wheel artery, and central scar was also assessed on ATPI images (Fig. 5). On ATPI, a central scar was defined as an area within the lesion that remained persistently nonenhancing throughout the analyzed time window.

Image analysis was independently performed by two ultrasound physicians with 10 years of experience in abdominal ultrasound. Both readers were blinded to the final diagnosis and other imaging findings. Disagreements were resolved by consensus or by consultation with a third senior reader.

# Statistical Analysis

Continuous variables are presented as the mean ± standard deviation and were compared using the independent-samples t test. Continuous variables with non-normal distribution were presented as median (interquartile range) and compared using the Mann–Whitney U test. Categorical variables are presented as numbers and percentages and were compared using the chi-square test or Fisher's exact test, as appropriate. HCA was defined as the positive diagnosis for the assessment of diagnostic performance. The diagnostic performance of CEUS alone and CEUS combined with ATPI for differentiating HCA from FNH was evaluated by calculating sensitivity, specificity, accuracy, positive predictive value, and negative predictive value. The McNemar test was used to compare the diagnostic accuracy between CEUS alone and CEUS combined with ATPI. Interobserver agreement between the two readers was assessed using Cohen's kappa statistic for CEUS diagnosis, CEUS-based vascular and structural features, ATPI-based vascular and structural features, and the final diagnosis based on CEUS combined with ATPI[13]. A two-sided P value of less than 0.05 was considered statistically significant. All statistical analyses were performed using SPSS software, version 26.0 (IBM Corp., Armonk, NY, USA).

## Results

# Participant Characteristics

A total of 54 patients with 54 lesions were included in this study, comprising 36 patients with FNH and 18 patients with HCA. Among these lesions, 9 were confirmed by histopathology, and 45 were diagnosed based on typical imaging findings on CECT or EOB-MRI with at least 12 months of follow-up. There were

no significant differences between the FNH and HCA groups in age, sex distribution, or liver background (all P > 0.05). The clinical characteristics of the patients are summarized in Table 1.

Table 1
Clinical characteristics of Focal Nodular Hyperplasia (FNH) and Hepatic Adenoma (HCA)

| **Characteristics** | **FNH (n = 36)** | **HCA (n = 18)** | ***P* value** |
|---|---|---|---|
| Age, mean ± SD | 41.14 ± 13.74 | 38.28 ± 12.30 | 0.459 |
| Sex, n (%) | | | 0.319 |
| Male | 15 (41.67%) | 5 (27.78%) | |
| Female | 21 (58.33%) | 13 (72.22%) | |
| Liver background, n (%) | | | 0.816 |
| Normal liver | 20 (55.56%) | 12 (66.67%) | |
| Liver cirrhosis | 3 (8.33%) | 1 (5.56%) | |
| Fatty liver | 13 (36.11%) | 5 (27.78%) | |

# Baseline sonographic features

The maximum lesion diameter was significantly larger in the FNH group than in the HCA group [31.00 (24.50, 44.00) mm vs. 18.00 (16.25, 33.50) mm, P = 0.047]. No significant differences were observed between the two groups in lesion depth, lesion location, echogenicity homogeneity, echogenicity, or lesion margin (all P > 0.05). The baseline ultrasound features of the lesions are shown in Table 2.

Table 2
Baseline ultrasound features of Focal Nodular Hyperplasia (FNH) and Hepatic Adenoma (HCA)

| **Baseline ultrasound features** | **FNH** | **HCA** | ***P* value** |
|---|---|---|---|
| Diameter of lesions, mm, median (Q1, Q3) | 31.00 (24.50,44.00) | 18.00 (16.25,33.50) | 0.047 |
| Lesion depth, mm, mean ± SD | 57.86 ± 21.18 | 52.33 ± 14.39 | 0.32 |
| Homogeneousness, n (%) | | | 0.19 |
| Homogeneous | 5 (13.89%) | 6 (33.33%) | |
| Inhomogeneous | 31 (86.11%) | 12 (66.67%) | |
| Echogenicity, n (%) | | | 0.42 |
| Isoechoic | 9 (25.00%) | 3 (16.67%) | |
| Hypoechoic | 26 (72.22%) | 13 (72.22%) | |
| Hyperechoic | 1 (2.78%) | 2 (11.11%) | |

# CEUS features

Regarding CEUS features, significant differences were observed between the FNH and HCA groups in arterial-phase enhancement pattern, the presence of a spoke-wheel artery on CEUS, and the presence of a central scar on CEUS (all $P < 0.05$). A spoke-wheel artery on CEUS was more frequently observed in FNH than in HCA [23/36 (63.89%) vs. 5/18 (27.78%), $P = 0.02$]. No significant differences were found in arterial-phase enhancement degree, portal venous-phase enhancement degree, late-phase enhancement degree, intralesional arterial branch on CEUS, or feeding artery on CEUS (all $P > 0.05$). Detailed CEUS features are presented in Table 3.

Table 3
CEUS features of Focal Nodular Hyperplasia (FNH) and Hepatic Adenoma (HCA)

| CEUS features | FNH | HCA | *P* value |
|---|---|---|---|
| Degree of arterial phase enhancement, n (%) | | | 0.41 |
| Isoenhancement | 2 (5.56%) | 3 (16.67%) | |
| Hyperenhancement | 34 (94.44%) | 15 (83.33%) | |
| Hypoenhancement | 0 (0.00%) | 0 (0.00%) | |
| Pattern of arterial phase enhancement, n (%) | | | 0.02 |
| Undetermined | 5 (13.89%) | 4 (22.22%) | |
| Homogeneous enhancement | 7 (19.44%) | 7 (38.89%) | |
| Centrifugal enhancement | 21 (58.33%) | 3 (16.67%) | |
| Centripetal enhancement | 3 (8.33%) | 4 (22.22%) | |
| Spoke-wheel artery, n (%) | | | 0.02 |
| Absent | 13 (36.11%) | 13 (72.22%) | |
| Present | 23 (63.89%) | 5 (27.78%) | |
| Intralesional arterial branch, n (%) | | | 0.39 |
| Absent | 13 (36.11%) | 9 (50.00%) | |
| Present | 23 (63.89%) | 9 (50.00%) | |
| Central scar, n (%) | | | 0.04 |
| Absent | 10 (27.78%) | 11 (61.11%) | |
| Present | 26 (72.22%) | 7 (38.89%) | |
| Feeding artery, n (%) | | | 0.85 |
| Absent | 19 (52.78%) | 9 (50.00%) | |
| Present | 17 (47.22%) | 9 (50.00%) | |
| Degree of portal venous phase enhancement, n (%) | | | 0.25 |
| Isoenhancement | 14 (38.89%) | 10 (55.56%) | |
| Hyperenhancement | 22 (61.11%) | 8 (44.44%) | |
| Hypoenhancement | 0(0.00%) | 0(0.00%) | |
| Degree of delayed phase enhancement, n (%) | | | 0.72 |
| Isoenhancement | 15 (41.67%) | 9 (50.00%) | |

| CEUS features | FNH | HCA | *P* value |
|---|---|---|---|
| Hyperenhancement | 14 (38.88%) | 5 (27.78%) | |
| Hypoenhancement | 7 (19.44%) | 4 (22.22%) | |

# ATPI features

Significant differences between FNH and HCA were observed in ATPI enhancement pattern, spoke-wheel artery, intralesional arterial branch, and feeding artery, whereas central scar on ATPI did not differ significantly between the two groups.

On ATPI, the enhancement pattern differed significantly between FNH and HCA. Centrifugal enhancement was the predominant pattern in the FNH group [31/36 (86.11%)], whereas centripetal enhancement was more frequently observed in the HCA group [13/18 (72.22%)]. A spoke-wheel artery on ATPI was identified in 27 of 36 FNH lesions (%) and in 3 of 18 HCA lesions (%), with a significant difference between the two groups ($P < 0.001$). An intralesional arterial branch on ATPI was more frequently observed in FNH than in HCA [24/36 (%) vs. 3/18 (16.67%), $P < 0.05$]. A feeding artery on ATPI was observed in 15 of 36 FNH lesions (41.67%) and 14 of 18 HCA lesions (77.78%), with a significant difference between the two groups ($P = 0.02$). In addition, a central scar on ATPI was observed in 24 of 36 FNH lesions (66.67%) and 15 of 18 HCA lesions (83.33%), with no significant difference between the two groups ($P = 0.33$). Detailed ATPI features are shown in Table 4.

Table 4
ATPI features of Focal Nodular Hyperplasia (FNH) and Hepatic Adenoma (HCA)

| ATPI features | FNH | HCA | *P* value |
|---|---|---|---|
| Pattern of arterial phase enhancement, n (%) | | | < 0.001 |
| Undetermined | 0 (0.00%) | 0 (0.00%) | |
| Homogeneous enhancement | 4 (11.11%) | 3 (16.67%) | |
| Centrifugal enhancement | 31 (86.11%) | 2 (11.11%) | |
| Centripetal enhancement | 1 (2.78%) | 13 (72.22%) | |
| Spoke-wheel artery, n (%) | | | < 0.001 |
| Absent | 9 (25.00%) | 15 (83.33%) | |
| Present | 27 (75.00%) | 3 (16.67%) | |
| Intralesional arterial branch, n (%) | | | 0.001 |
| Absent | 12 (33.33%%) | 15 (83.33%) | |
| Present | 24 (66.67%) | 3 (16.67%) | |
| Central scar, n (%) | | | 0.33 |
| Absent | 24 (66.67%) | 15 (83.33%) | |
| Present | 12 (33.33%) | 3 (16.67%) | |
| Feeding artery, n (%) | | | 0.02 |
| Absent | 21 (58.33%) | 4 (22.22%) | |
| Present | 15 (41.67%) | 14 (77.78%) | |

# Diagnostic performance of CEUS and CEUS combined with ATPI

With HCA defined as the positive diagnosis, the diagnostic performance of CEUS alone and CEUS combined with ATPI was assessed based on the consensus interpretation. CEUS alone showed a sensitivity of 77.8%, specificity of 86.1%, accuracy of 83.3%, PPV of 73.7%, and NPV of 88.6% for differentiating HCA from FNH. After ATPI was incorporated into the diagnostic assessment, the sensitivity, specificity, accuracy, PPV, and NPV were 94.4%, 91.7%, 92.6%, 85%, and 97.1%, respectively. The diagnostic accuracy increased from 83.3% with CEUS alone to 92.6% with CEUS combined with ATPI, although the difference was not statistically significant (P = 0.12, McNemar test). Detailed results are presented in Table 5.

Table 5
Diagnostic performance of CEUS alone and CEUS combined with ATPI

| Method | Se | Sp | PPV | NPV | Accuracy | *P* value |
|---|---|---|---|---|---|---|
| CEUS alone | 77.8% | 86.1% | 73.7% | 88.6% | 83.3% | 0.12 |
| CEUS + ATPI | 94.4% | 91.7% | 85% | 97.1% | 92.6% | |

HCA was defined as the positive diagnosis. *P* values were calculated using the McNemar test to compare diagnostic accuracy between CEUS alone and CEUS combined with ATPI. Se, Sensitivity; Sp, Specificity; PPV, Positive Predictive Value; NPV, Negative Predictive Value

# Interobserver agreement

The two readers showed substantial agreement in the diagnosis of FNH and HCA based on CEUS alone (κ = 0.683). After ATPI was incorporated into the diagnostic assessment, interobserver agreement increased to κ = 0.757, indicating substantial agreement. Interobserver agreement for CEUS and ATPI features, including enhancement patterns, enhancement degree, spoke-wheel artery, nourishing artery, feeding artery, and central scar, is summarized in Supplementary Table 1.

# Discussion

In this study, ATPI provided additional information for differentiating FNH from HCA by visualizing early arterial perfusion patterns and intralesional vascular architecture. Specifically, FNH more commonly showed centrifugal enhancement on ATPI, whereas HCA more frequently showed centripetal enhancement. Spoke-wheel arteries and intralesional arterial branches were more frequently identified in FNH. Incorporating ATPI with CEUS resulted in a trend toward improved diagnostic performance compared with CEUS alone. Furthermore, ATPI also increased interobserver agreement for both diagnostic assessment and evaluation of vascular features.

In the present cohort, baseline clinical characteristics were comparable between the FNH and HCA groups, whereas lesion size differed significantly. This difference should be interpreted cautiously because of the relatively small sample size and the retrospective nature of the study, which may have introduced selection bias[14].

The most prominent ATPI finding in this study was the difference in enhancement direction between FNH and HCA. Most FNH lesions showed centrifugal enhancement, whereas most HCA lesions showed centripetal enhancement. This difference may reflect their distinct vascular architectures. Classic FNH is characterized by a central feeding artery and radiating fibrous septa, which may correspond to the centrifugal perfusion pattern and spoke-wheel vascular appearance on ATPI[2]. In contrast, HCA lacks the typical central scar and spoke-wheel vascular architecture of FNH, which may explain the more frequent centripetal or heterogeneous enhancement pattern[15]. The higher frequency of feeding arteries observed in HCA may be related to the hypervascular nature of these lesions and their arterial blood supply[16]. Unlike FNH, which often shows a central arterial supply with radiating intralesional branches[17], HCA may

more frequently demonstrate a relatively prominent arterial vessel entering the lesion from the surrounding liver parenchyma[18]. ATPI may facilitate visualization of the feeding artery and intralesional arterial branches through color-coding the temporal sequence of microbubble arrival.

Although central scar differed significantly between FNH and HCA on CEUS, the difference was not significant on ATPI. One possible explanation is that ATPI in this study was generated from only the first 5 seconds after contrast arrival in the lesion. Central scars may become more conspicuous during later CEUS phases[11]; therefore, scars appearing outside the selected early arterial time window may not be adequately captured by ATPI. These findings suggest that ATPI may be particularly useful for depicting early arterial perfusion direction and vascular architecture, whereas its ability to demonstrate central scar may be limited by the selected time window.

In terms of diagnostic performance, the addition of ATPI to CEUS improved sensitivity, specificity, accuracy, PPV, and NPV for differentiating HCA from FNH in this cohort. Although CEUS combined with ATPI showed higher diagnostic indices than CEUS alone, the improvement in diagnostic accuracy did not reach statistical significance. This may be partly attributable to the limited sample size, particularly the relatively small number of HCA lesions[19]. Nevertheless, ATPI provided additional information on early arterial enhancement patterns and vascular architecture, which may be useful as an adjunct to CEUS[20]. The diagnostic performance of CEUS alone in the present study was lower than that reported in some previous studies[10,21]. This discrepancy may be related to differences in study populations, lesion types, diagnostic criteria, reader experience, and the proportion of atypical lesions. ATPI also improved interobserver agreement in this study. Compared with conventional CEUS interpretation, color-coded ATPI provided a more intuitive display of enhancement direction and vascular architecture[22], including spoke-wheel arteries, intralesional arterial branches, and feeding arteries. This may explain the increased agreement between the two readers when ATPI was incorporated into the diagnostic process.

To our knowledge, few studies have specifically evaluated the early arterial ATPI features of FNH and HCA[8]. The present study suggests that ATPI may provide additional information on enhancement direction and vascular architecture within the first 5 seconds after contrast arrival, thereby improving the differentiation of these two lesions when combined with CEUS.

This study has several limitations. First, it was a retrospective single-center study with a relatively small sample size, particularly for HCA. Second, not all lesions were confirmed histopathologically; some were diagnosed based on CECT or EOB-MRI findings with imaging follow-up, which may have introduced verification bias. Third, ATPI analysis was performed only using the early arterial phase within 5 seconds after contrast arrival, and portal venous- and late-phase ATPI were not evaluated. Finally, HCA subtypes were not analyzed, although different molecular subtypes may have distinct imaging features.

# Conclusions

In conclusion, ATPI may improve visualization of early arterial enhancement patterns and vascular architecture in FNH and HCA. When combined with CEUS, ATPI may improve interobserver agreement for differentiating HCA from FNH. Its incremental diagnostic benefit requires validation in prospective multicenter studies with larger sample size.

## List of abbreviations

Focal nodular hyperplasia (FNH)

Hepatocellular adenoma (HCA)

Arrival-time parametric imaging (ATPI)

Contrast-enhanced ultrasound (CEUS)

Contrast-enhanced computed tomography (CECT)

Gadoxetic acid-enhanced magnetic resonance imaging (EOB-MRI)

## Declarations

**Ethics approval and consent to participate**

This study was approved by the Ethics Committee of The First Hospital of Jilin University (AF-IRB-032-06). All procedures involving human participants were performed in accordance with the ethical standards laid down in the Declaration of Helsinki and its later amendments.

**Consent for publication**

Not Applicable.

# Competing interests

The authors declare that they have no conflicts of interest relevant to this study.

# Funding

This work was supported by the Jilin Provincial Natural Science Foundation General Project (Grant No. YDZJ202601ZYTS605).

# Author Contribution

Zhang DZ, Qin XY and Li QX conceived and designed the study. Zhu YP, He HB and Zheng Q collected the data. Sun Y, Wang DX and Sui MW analyzed the data. Qin XY drafted the manuscript. Li QX and Zhang DZ revised the manuscript. All authors read and approved the final manuscript.


# Acknowledgement

We extend our thanks to Ping Ji and Jing Zhang from GE Healthcare for providing us with training on the operation of arrival-time parametric imaging.


# Data Availability

The datasets used or analysed during the current study are available from the corresponding author on reasonable request.

## References


1. Frenette C, Mendiratta-Lala M, Salgia R, et al. ACG Clinical Guideline: Focal Liver Lesions. Am J Gastroenterol. 2024;119(7):1235–71. 10.14309/ajg.0000000000002857.
2. Villavicencio Kim J, Wu GY. Focal Nodular Hyperplasia: A Comprehensive Review with a Particular Focus on Pathogenesis and Complications. J Clin Translational Hepatol. 2024;12(2):182–90. 10.14218/JCTH.2023.00265.
3. Poetter-Lang S, Ba-Ssalamah A, Bastati N, et al. Hepatocellular adenoma update: diagnosis, molecular classification, and clinical course. Br J Radiol. 2024;97(1163). 10.1093/bjr/tqae180.
4. EASL Clinical Practice Guidelines on the management of benign liver tumours. J Hepatol. 2016;65(2):386–98. 10.1016/j.jhep.2016.04.001.
5. Reguram R, Ghonge A, Tse J, Dhanasekaran R. Practical approach to diagnose and manage benign liver masses. Hepatol Commun. 2024;8(11):e0560. 10.1097/HC9.0000000000000560.
6. Myers L, Ahn J. Focal Nodular Hyperplasia and Hepatic Adenoma: Evaluation and Management. Clin Liver Dis. 2020;24(3). 10.1016/j.cld.2020.04.013.
7. Bastati-Huber N, Pötter-Lang S, Ba-Ssalamah A. Fokale noduläre Hyperplasie und hepatozelluläres Adenom [Focal nodular hyperplasia and hepatocellular adenoma]. Radiologe. 2015;55(1):18–26. 10.1007/s00117-014-2704-9.
8. Jiang N, Cao JY, Jin Z, Yu TQ, Chen ST, Zhang Y. Enhanced Diagnostic Imaging: Arrival-Time Parametric Imaging in Contrast-Enhanced Ultrasound for Multi-Organ Assessment. Med Sci Monit. 2024;30:e945281. 10.12659/MSM.945281.
9. Lupușoru R, Sporea I, Rațiu I, et al. Contrast-Enhanced Ultrasonography with Arrival Time Parametric Imaging as a Non-Invasive Diagnostic Tool for Liver Cirrhosis. Diagnostics (Basel Switzerland). 2022;12(12). 10.3390/diagnostics12123013.

10. Bröker MEE, Taimr P, de Vries M, et al. Performance of Contrast-Enhanced Sonography Versus MRI With a Liver-Specific Contrast Agent for Diagnosis of Hepatocellular Adenoma and Focal Nodular Hyperplasia. AJR Am J Roentgenol. 2020;214(1). 10.2214/AJR.19.21251.
11. Dietrich CF, Nolsøe CP, Barr RG et al. Guidelines and Good Clinical Practice Recommendations for Contrast Enhanced Ultrasound (CEUS) in the Liver - Update 2020 - WFUMB in Cooperation with EFSUMB, AFSUMB, AIUM, and FLAUS. *Ultraschall in der Medizin (Stuttgart, Germany: 1980)*. 2020;41(5). 10.1055/a-1177-0530
12. Yen YH, Wang JH, Lu SN, et al. Contrast-enhanced ultrasonographic spoke-wheel sign in hepatic focal nodular hyperplasia. Eur J Radiol. 2006;60(3). 10.1016/j.ejrad.2006.06.007.
13. Landis JR, Koch GG. The measurement of observer agreement for categorical data. Biometrics. 1977;33(1).
14. Grimes DA, Schulz KF. Bias and causal associations in observational research. Lancet. 2002;359(9302):248–52. 10.1016/S0140-6736(02)07451-2.
15. Cannella R, Brancatelli G, Rangaswamy B, Minervini MI, Borhani AA, Furlan A. Enhancement pattern of hepatocellular adenoma (HCA) on MR imaging performed with Gd-EOB-DTPA versus other Gd-based contrast agents (GBCAs): An intraindividual comparison. Eur J Radiol. 2019;119:108633. 10.1016/j.ejrad.2019.08.002.
16. Poetter-Lang S, Ba-Ssalamah A, Bastati N, et al. Hepatocellular adenoma update: diagnosis, molecular classification, and clinical course. Br J Radiol. 2024;97(1163):1740–54. 10.1093/bjr/tqae180.
17. Jang JY, Kim MY, Jeong SW, et al. Current consensus and guidelines of contrast enhanced ultrasound for the characterization of focal liver lesions. Clin Mol Hepatol. 2013;19(1):1–16. 10.3350/cmh.2013.19.1.1.
18. Khanna M, Ramanathan S, Fasih N, Schieda N, Virmani V, McInnes MDF. Current updates on the molecular genetics and magnetic resonance imaging of focal nodular hyperplasia and hepatocellular adenoma. Insights Imaging. 2015;6(3):347–62. 10.1007/s13244-015-0399-8.
19. Hajian-Tilaki K. Sample size estimation in diagnostic test studies of biomedical informatics. J Biomed Inf. 2014;48:193–204. 10.1016/j.jbi.2014.02.013.
20. Denis de Senneville B, Frulio N, Laumonier H, Salut C, Lafitte L, Trillaud H. Liver contrast-enhanced sonography: computer-assisted differentiation between focal nodular hyperplasia and inflammatory hepatocellular adenoma by reference to microbubble transport patterns. Eur Radiol. 2020;30(5):2995–3003. 10.1007/s00330-019-06566-1.
21. Şirli R, Sporea I, Popescu A, et al. Contrast-enhanced ultrasound for the assessment of focal nodular hyperplasia - results of a multicentre study. Med Ultrason. 2021;23(2):140–6. 10.11152/mu-2912.
22. Wakui N, Takayama R, Kamiyama N, et al. Arrival time parametric imaging using Sonazoid-enhanced ultrasonography is useful for the detection of spoke-wheel patterns of focal nodular hyperplasia smaller than 3 cm. Experimental Therapeutic Med. 2013;5(6):1551–4. 10.3892/etm.2013.1048.

# Figures

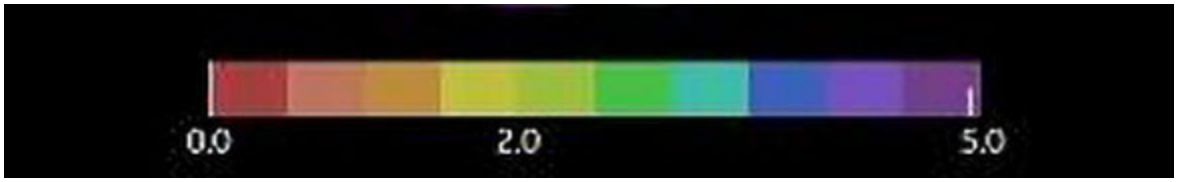



**Figure 1**

Color-coded schematic of ATPI. The color bar indicates the time intervals: red (0-0.5 s), orange-red (0.5-1.0 s), orange (1.0-1.5 s), yellow (1.5-2.0 s), yellow-green (2.0-2.5 s), green (2.5-3.0 s), blue-green (3.0-3.5 s), blue (3.5-4.0 s), violet (4.0-4.5 s), and purple (4.5-5.0 s).

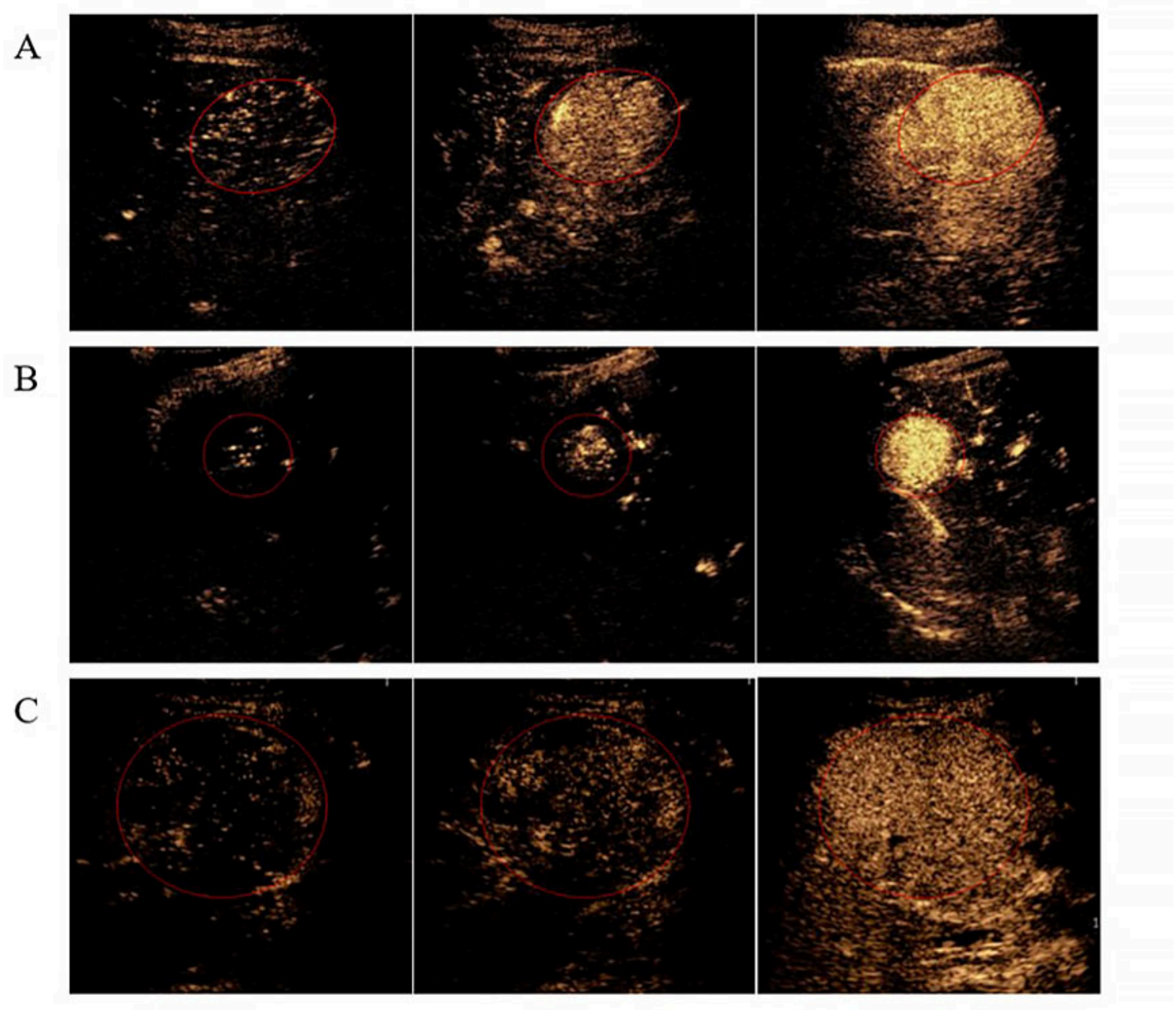


**Figure 2**

Enhancement patterns during the arterial phase of CEUS. (A) Homogeneous enhancement; (B) Centrifugal enhancement; (C) Centripetal enhancement.

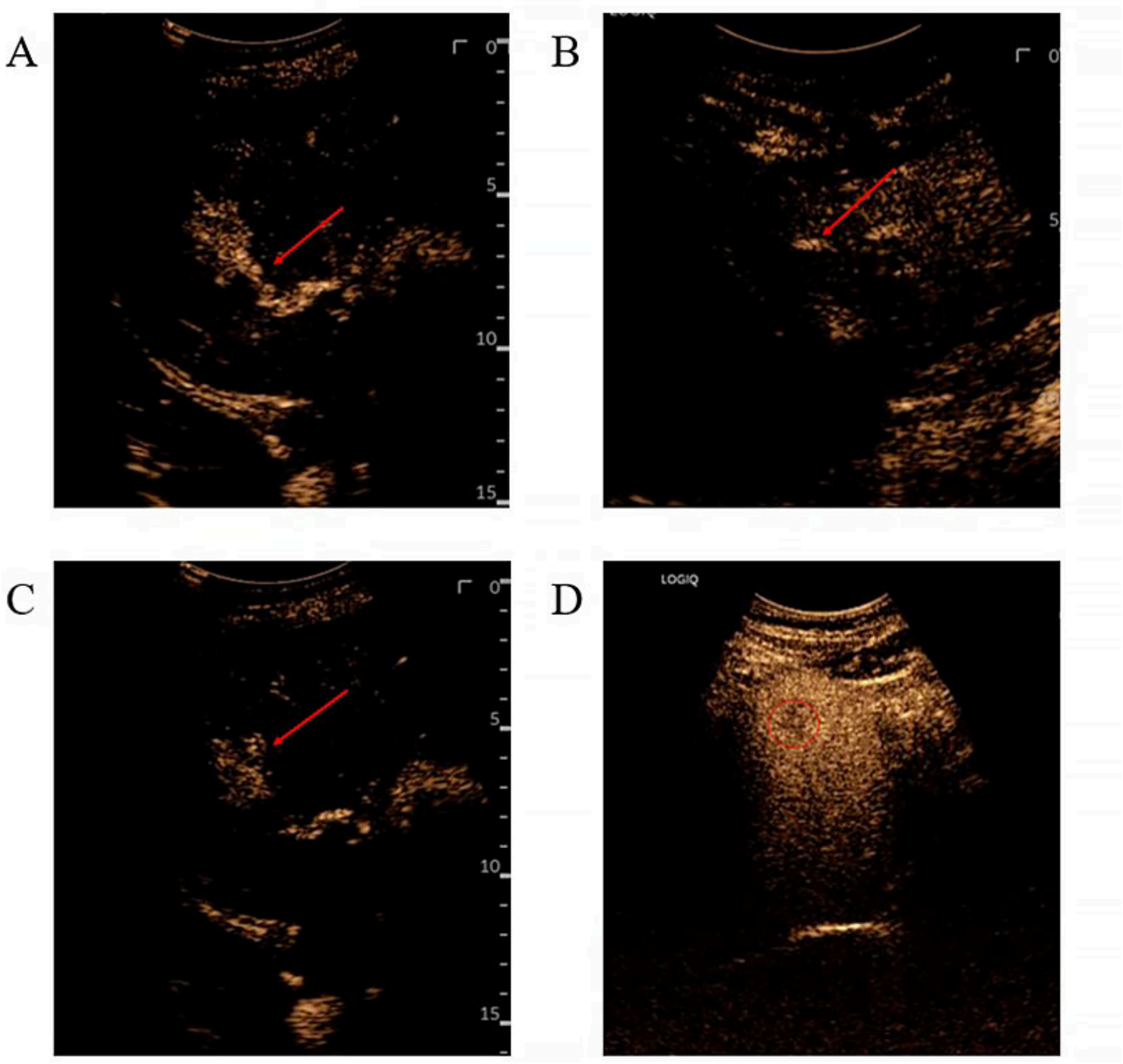



**Figure 3**

Characteristic CEUS findings of the lesion. (A) Peritumoral feeding artery supplying the mass; (B) Intratumoral vessels originating from the feeding artery; (C) Spoke-wheel sign with radial vascular

distribution; (D) Avascular central scar showing no enhancement.

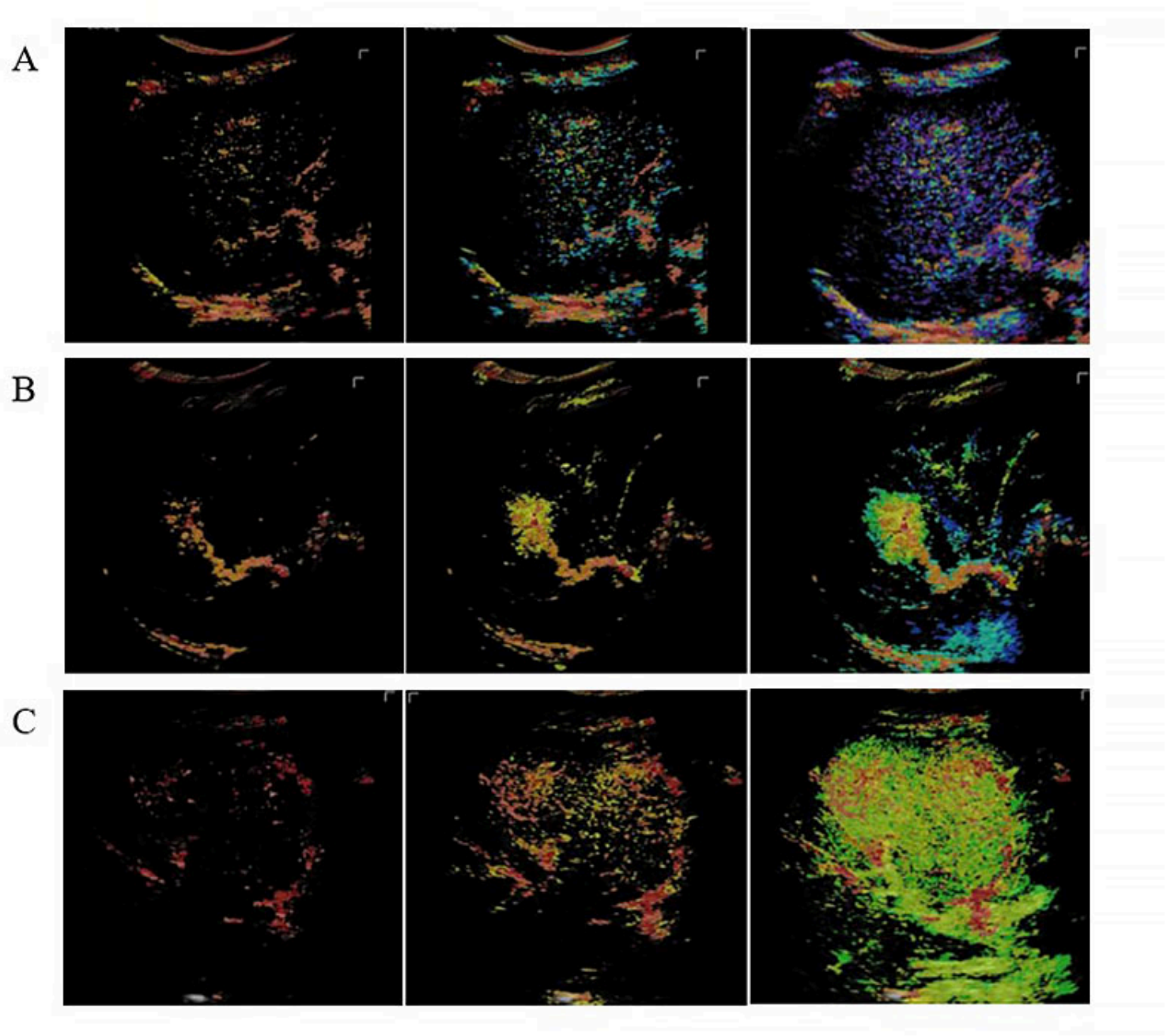



**Figure 4**

Enhancement patterns during the arterial phase of ATPI. (A) Homogeneous enhancement; (B) Centrifugal enhancement; (C) Centripetal enhancement.

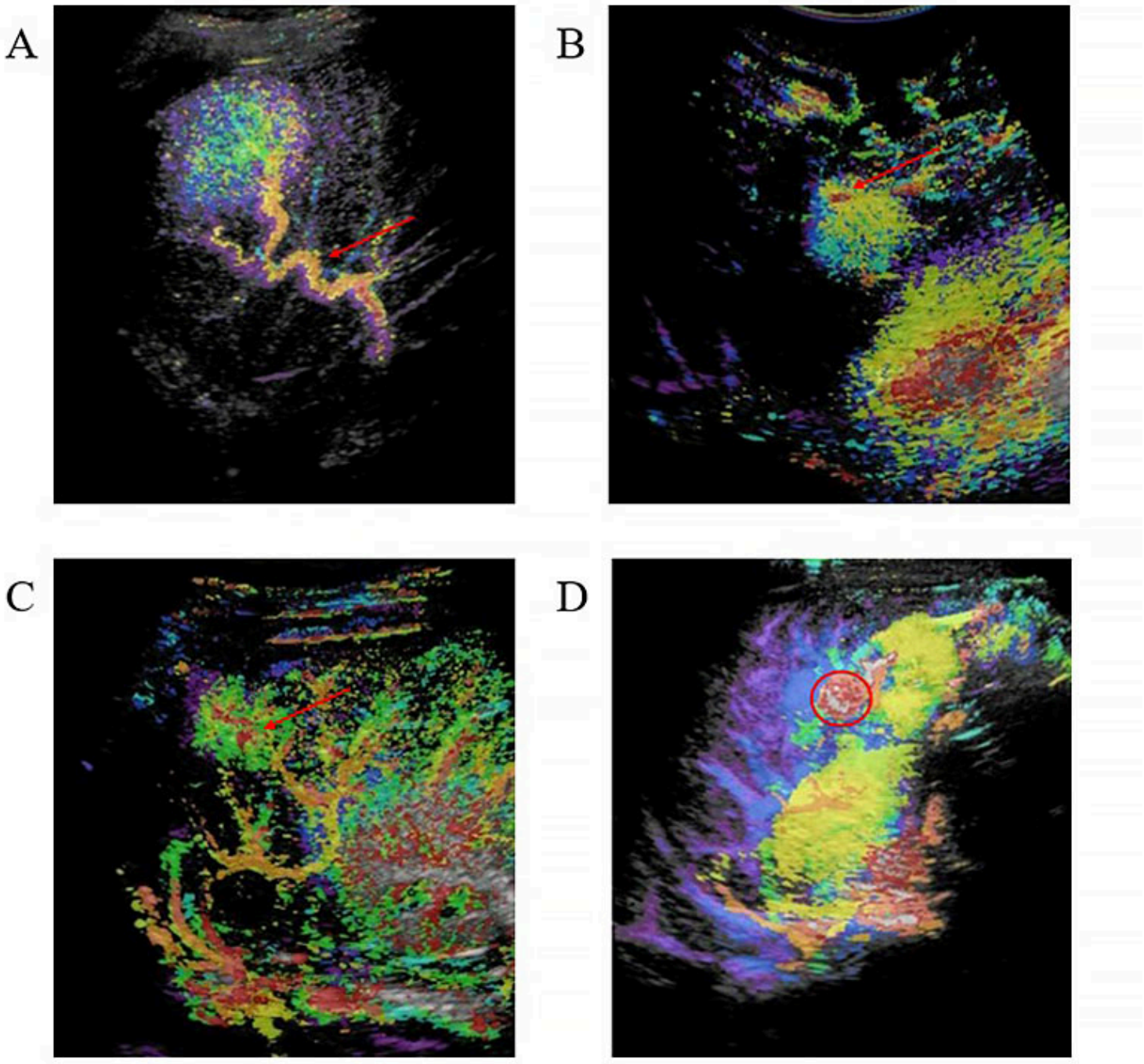



**Figure 5**

Vascular and structural features of the lesion on ATPI. (A) Feeding artery; (B) Intralesional nourishing branch; (C) Spoke-wheel artery; (D) Central scar.

## Supplementary Files

This is a list of supplementary files associated with this preprint. Click to download.

- SupplementaryMaterial.docx